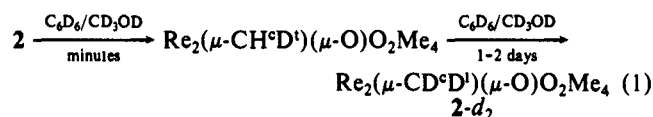


Re-Re σ bond and two electrons in a nonbonded orbital concentrated on the octahedral Re center; thus, the molecule is best described as a mixed-valent "d³-d¹ complex".

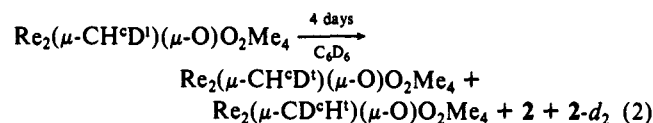
The lone pair of electrons on the octahedral center suggested that oxidation of **1** was feasible. Addition of 3 equiv of pyridine *N*-oxide to a blue toluene solution of **1** resulted in a slow color change of the solution to orange and the precipitation of a white solid (Me₃PO). The orange solution was filtered through an alumina pad (grade V) to remove Me₃PO, and subsequent crystallization from toluene at -80 °C gave orange plates of diamagnetic d¹-d¹ Re₂(μ -CH₂)(μ -O)O₂Me₄ (**2**) in 75% yield.¹²

The structure of **2** (ORTEP, Figure 1)^{9,13} resembles those of the d¹-d¹ dimers [Re(μ -O)(O)R₂]₂ (R = Me, CH₂CMe₃, or CH₂CMe₂Ph),^{2a,10} for which each Re center has a square-pyramidal geometry with a terminal oxo ligand in the apical position. The Re-Re distance (2.654 (2) Å) is consistent with a single bond (cf. Re-Re = 2.593 (1) Å in [Re(μ -O)(O)Me₂]₂).^{2a}

The reaction of **2** in benzene-*d*₆ with methanol-*d*₄ (100 equiv) resulted in deuterium incorporation into both methylene proton sites (eq 1). The rates of deuterium incorporation were markedly different for the two inequivalent sites, with the incorporation much more rapid (minutes vs days) at the proton position trans with respect to the terminal oxo ligands (H^t) than at the cis position (H^c). The addition of 100 equiv of glacial acetic acid-*d*₄ to **2** in benzene-*d*₆, followed immediately by 100 equiv of methanol-*d*₄, resulted in a relatively much slower deuterium enrichment at both sites, indicating that acid inhibits the deuterium exchange reaction.



In related experiments, an approximately 1:1 mixture of Re₂(μ -CD₂)(μ -O)O₂Me₄ (*2-d*₂) and **2** in benzene-*d*₆ within minutes of preparation gave an \approx 1:1:1:1 mixture of **2**, *2-d*₂, Re₂(μ -CH^cD^t)(μ -O)O₂Me₄, and Re₂(μ -CD^cH^t)(μ -O)O₂Me₄. The crossover was slowed by the addition of acetic acid-*d*₄. Additionally, Re₂(μ -CH^cD^t)(μ -O)O₂Me₄ alone in benzene-*d*₆ gave the four possible H/D products (\approx 1:1:1:1 ratio) on standing for 4 days (eq 2). It is not clear in this experiment, nor in the reactions involving methanol as a deuterium source, whether the deuterium incorporation into the H^c position is via inter or intramolecular processes.



These facile deuterium crossover and exchange reactions suggested that deprotonation of **2** was feasible. Thus, the reaction of **2** with 1 equiv of LiCH₂CMe₃ in pentane gave neopentane and Li[Re₂(μ -CH)(μ -O)O₂Me₄] (**3**; Figure 1) as a hydrocarbon-insoluble orange powder in 85% yield.¹⁴ The reaction of Re₂(μ -

CH^cD^t)(μ -O)O₂Me₄ with 1 equiv of LiCH₂CMe₃ gave only protio **3** by NMR integration (i.e., no Li[Re₂(μ -CD)(μ -O)O₂Me₄]).

A mechanism involving virtual dissociation of **2** to **3** and H⁺, perhaps with another molecule of **2** acting as the base in the crossover experiments, would account for the fast deuterium incorporation and crossover observed at the methylene H^t position, and the acid inhibition. The basic site in **2** would likely be the bridging oxo group (cf. [Re(μ -O)OCp*]₂ + 2H⁺ → [[Re(μ -OH)OCp*]₂]²⁺).¹⁵

One component of an alternative mechanism is illustrated in eq 3. In this case, the fast H^t/D incorporation and crossover would Re₂(μ -CH^tH^t)(μ -O)O₂Me₄ \rightleftharpoons Re₂(μ -CH^c)(μ -OH^t)O₂Me₄ (**3**)

occur via a bridging hydroxide, which results from a 1,3-shift of the H^t methylene proton to the bridging oxo ligand in **2**, and charged species would not necessarily be involved. Acid would inhibit the equilibrium by binding to the bridging oxo group in **2**. In eq 3 the proton transfer would result in the formation of partial Re-(μ -CH) multiple bonds without significant loss of Re-(μ -O) multiple bonding, providing a driving force for the transfer.^{4a,16}

Acknowledgment is made to the donors of the Petroleum Research Fund, administered by the American Chemical Society, for the support of this research.

Supplementary Material Available: Procedures for the X-ray structure determinations, complete tables of bond distances and angles, atomic coordinates, non-hydrogen atom anisotropic displacement parameters, packing diagrams, and ORTEP plots showing the atom-numbering schemes for **1** and **2** (25 pages); listing of observed and calculated structure factors for **1** and **2** (28 pages). Ordering information is given on any current masthead page.

(14) Amounts used in a typical preparation: LiCH₂CMe₃ (0.006 g, 0.08 mmol); **2** (0.038 g, 0.08 mmol); pentane (20 mL). ¹H NMR (CD₃CN): δ 12.23 (s, 1, μ -CH), 2.10 (s, 6, CH₃), 1.35 (s, 6, CH₃). ¹³C NMR (CD₃CN): δ 258.4 (d, 1, J_{CH} = 183 Hz, μ -CH), 25.7 (q, 2, J_{CH} = 125 Hz, CH₃), 19.0 (q, 2, J_{CH} = 128 Hz, CH₃). IR (Nujol, CsI, cm⁻¹): ν (Re=O) 981 s, 967 m, ν (asym ReORe) 668 w.

(15) Herrmann, W. A.; Küsthardt, U.; Floël, M.; Kulpe, J.; Herdtweck, E.; Voss, E. *J. Organomet. Chem.* **1986**, *314*, 151.

(16) Related work: Rocklage, S. M.; Schrock, R. R.; Churchill, M. R.; Wasserman, H. J. *Organometallics* **1982**, *1*, 1332. Freudenberger, J. H.; Schrock, R. R. *Organometallics* **1985**, *4*, 1937.

Hydration of Cavities in Proteins: A Molecular Dynamics Approach

Rebecca C. Wade,*† Michael H. Mazon,†
J. Andrew McCammon,† and Florante A. Quioccho†

Department of Chemistry, University of Houston
Houston, Texas 77204-5641
Howard Hughes Medical Institute, Departments of
Biochemistry and of Physiology and Molecular Biophysics
Baylor College of Medicine, Houston, Texas 77030

Received May 4, 1990

Internal water molecules play an important role in the structure and function of proteins.¹⁻⁵ The ability to predict their structural and thermodynamic properties would be of value in, e.g., the design of ligands, such as drugs; the study of protein-protein interfaces and protein folding; and the location of water molecules in protein structures solved at low resolution by X-ray crystallography.

*University of Houston.

†Baylor College of Medicine.

(1) Edsall, J. T.; McKenzie, H. A. *Adv. Biophys.* **1983**, *16*, 53-184.
(2) Finney, J. L. In *Water: A Comprehensive Treatise*; Franks, F., Ed.; Plenum: New York, 1979; Vol. 6, pp 47-122.

(3) Baker, E. N.; Hubbard, R. E. *Prog. Biophys. Mol. Biol.* **1984**, *44*, 97-180.

(4) Saenger, W. *Annu. Rev. Biophys. Biophys. Chem.* **1987**, *16*, 93-114.

(5) Rashin, A. A.; Iofin, M.; Honig, B. *Biochemistry* **1986**, *25*, 3619-3625.

(12) Amounts used in a typical preparation: pyridine *N*-oxide (0.070 g, 0.074 mmol); **1** (0.155 g, 0.240 mmol); toluene (30 mL).

(13) Anal. Calcd for Re₂O₃C₅H₁₄: C, 12.14; H, 2.85. Found: C, 12.42; H, 2.77. By ¹H NMR, **2** has C₂ symmetry in solution. ¹H NMR (C₆D₆): δ 9.49 (d, 1, J_{HH} = 14.5 Hz, μ -CH₂H_b trans with respect to Re=O), 6.01 (d, 1, J_{HH} = 14.5 Hz, μ -CH₂H_a cis with respect to Re=O). ¹³C NMR (C₆D₆): δ 158.1 (dd, 1, J_{CHa} = 161 Hz, J_{CHb} = 131 Hz, μ -CH₂). IR (Nujol, CsI, cm⁻¹): ν (Re=O) 1014 s, 1001 m, ν (asym ReORe) 748 w (ν (Re¹⁸O₃) 973, 960, 720). Crystal data for C₅H₁₄O₃Re₂ at -76 (1) °C: orange plates, 0.20 × 0.20 × 0.10 mm, triclinic, space group P1, *a* = 5.853 (3) Å, *b* = 5.912 (2) Å, *c* = 15.895 (7) Å, α = 89.72 (4)°, β = 85.34 (5)°, γ = 60.52 (3)°, *d*_{calcd} = 3.44 g cm⁻³, *Z* = 2, μ = 256.7 cm⁻¹. X-ray diffraction data were collected on a Nicolet R3m/V diffractometer using graphite-monochromated Mo K α radiation (λ = 0.71073 Å) in the θ -2 θ scan mode. A semiempirical absorption correction (XEMP) and Lorentz and polarization corrections were applied to the data. A total of 2339 reflections were collected in the range 4° < 2 θ < 50° (*h*, \pm *k*, \pm *l*); 1646 were unique reflections (*R*_{int} = 0.056), and 1383 with *F*_o > 6 σ (*F*_o) were used in the structure solution. *R*(*F*) = 0.0450; *R*_w(*F*) = 0.0475.

Table I. Free Energy Changes (kcal/mol) for the Introduction of a Water Molecule into Pure Water and into Two Cavities in SBP^a

energy component	theor ΔA for pure water	exptl ΔG for pure water ^b	theor ΔA for hydrated cavity in SBP	theor ΔA for "dry" cavity in SBP
electrostatic ^c	$-8.4 \pm 0.3^{d,e}$	-8.7	-11.9 ± 0.9	-1.9 ± 0.9
Lennard-Jones	2.0 ± 0.1	2.4	-4.5 ± 0.0	-4.3 ± 0.2
total	-6.4 ± 0.4^f	-6.3	-16.4 ± 0.9	-6.2 ± 1.1

^aMolecular dynamics simulations were performed by using the GROMOS program²⁴ and the SPC/E model for water.²⁵ Covalent bonds were constrained by using SHAKE.²⁶ The masses of all hydrogens in the SBP systems were increased to 10 amu,²⁷ allowing a time step of 5 fs to be used once the system was equilibrated. In the SBP systems, the mass of the oxygen of the perturbed water molecule was increased to 90 000 amu to prevent it from leaving the protein cavity during TI. The electrostatic and Lennard-Jones components of ΔA were computed in separate simulations of length 80–250 ps. Simulations were run in forward and reverse directions with more sampling in regions where the free energy showed faster variation. In the SBP systems, when the coupling of the perturbed water molecule was such that it was equivalent to a very small uncharged particle, free energies were obtained by using TPT with 10-ps equilibration and 10-ps data collection for 1–2 windows. ^bFrom measurements of vapor pressure and density for water and noble gases.²⁸ ^cAfter subtraction of a 1.25 kcal/mol polarization energy correction term.²⁵ ^dThis free energy was also calculated by TPT and by TI in the isothermal, isobaric ensemble (M.H.M., unpublished results). Its error was estimated as the standard deviation of the free energies from all the TI and TPT simulations. Errors for all other free energies were estimated from the hysteresis between forward and reverse runs in the TI simulations. ^eJorgensen et al.¹⁷ have computed a $\Delta G = -8.4$ kcal/mol for the perturbation of a methane molecule into a TIP4P water molecule²⁹ in pure water. ^fHermans et al.¹⁶ have computed a $\Delta A = -5.5$ kcal/mol for SPC/E water²⁵ and Jorgensen et al.¹⁷ have computed a $\Delta G = -6.1 \pm 0.3$ kcal/mol for TIP4P water.²⁹

Numerous theoretical methods have been used to study protein hydration.^{5–13} Here, we propose the application of statistical thermodynamic perturbation and integration techniques to determine the energetic and structural properties of internal water molecules in proteins. These techniques have previously been used for computing the excess chemical potential of water^{14–17} and the relative free energies of hydration of small molecules and ions (see, for example, refs 17–19). The excess chemical potential of water is constant throughout a system at equilibrium and is given by the free energy change associated with hydrating any given position in bulk solvent with one water molecule. Protein cavities will tend to be occupied by water if the corresponding free energy of hydration is less than that of the bulk solvent. This free energy has been computed for two representative cavities in a protein and found to be consistent with their experimentally observed occupancies.

The free energy of hydration of a cavity with one water molecule may be given by the sum of the free energy changes for two processes: (1) the removal of a water molecule from pure water and (2) the introduction of a water molecule into the cavity. These free energy changes may be calculated by using thermodynamic perturbation theory (TPT)²⁰ and thermodynamic integration methods (TI).²¹

The hydration of two internal cavities in a sulfate-binding protein (SBP) was studied. The structure of the SBP from *Salmonella typhimurium* has been solved by X-ray crystallography to 1.7 Å resolution and an *R*-factor of 14%,^{22,23} and

therefore, SBP provided a suitable model system. The cavities were chosen so that one, representative of a hydrated cavity, contained a single crystallographic water while the other, representative of an unhydrated cavity, was "dry" and contained no crystallographic waters.

Three sets of TI simulations were carried out (see footnote a, Table I) for the perturbation of a single water molecule at the center of an 18-Å sphere of equilibrated atoms, with atoms in the outer 8-Å shell harmonically constrained to their initial coordinates. The spheres of atoms were cut, in turn, from a box of equilibrated waters; from the solvated protein centered on the crystallographically observed water in the chosen hydrated cavity; and from the solvated protein centered on a dummy water molecule in the "dry" cavity.

The results are given in Table I. The Helmholtz free energies (ΔA) computed for pure water show good agreement with Gibbs free energies (ΔG) derived from experimental observations²⁸ and with other recent calculations of these free energies^{16,17} (see footnotes d–f, Table I).

In SBP, the magnitude of the electrostatic component of ΔA is greater in the hydrated cavity than in the pure water system whereas, in the "dry" cavity, it is less. This is due to differences in the structural properties of the surrounding atoms and in the number of hydrogen bonds formed by the perturbed water molecule. The water molecule in the hydrated cavity could make four hydrogen bonds which were broken as the partial charges were removed and were reformed when they were replaced. The dummy water molecule in the "dry" cavity could only make two weak hydrogen bonds to the protein.

The Lennard-Jones component of ΔA is similar in magnitude for the two protein cavities and, compared to that for pure water, larger and of opposite sign. This is because, in the pure water system, the surrounding water molecules were able to collapse into the cavity created by the vanishing perturbed water molecule whereas, in SBP, the protein atoms were unable to reorder to fully occupy the empty cavities.

For the hydrated cavity, the calculated Helmholtz free energy of hydration (ΔA_{hyd}) is -10.0 ± 1.3 kcal/mol, corresponding to an equilibrium binding constant $K_{\text{eq}} \approx 10^7$ and approximately unit occupancy. In contrast, for the "dry" cavity, $\Delta A_{\text{hyd}} = 0.2 \pm 1.5$ kcal/mol, showing that this cavity is likely to be unoccupied. The

(6) Richards, W. G.; King, P. M.; Reynolds, C. A. *Protein Eng.* **1989**, *2*, 319–327.

(7) Lee, B.; Richards, F. M. *J. Mol. Biol.* **1971**, *119*, 379–400.

(8) Goodford, P. J. *J. Med. Chem.* **1985**, *28*, 849–857.

(9) Wade, R. C. *J. Comput. Aided Mol. Des.* **1990**, *4*, 199–204.

(10) Finney, J. L.; Goodfellow, J. M.; Howell, P. L.; Vovelle, F. *J. Biomol. Struct. Dyn.* **1985**, *3*, 599–622.

(11) Levitt, M.; Sharon, R. *Proc. Natl. Acad. Sci. U.S.A.* **1988**, *85*, 7557–7561.

(12) Brooks, C. L.; Karplus, M. *J. Mol. Biol.* **1989**, *208*, 159–181.

(13) Pullman, A.; Pullman, B. *Q. Rev. Biophys.* **1975**, *7*, 505–566.

(14) Mezei, M.; Swaminathan, S.; Beveridge, D. L. *J. Am. Chem. Soc.* **1978**, *100*, 3255–3256.

(15) Mezei, M. *Mol. Phys.* **1982**, *47*, 1307–1315.

(16) Hermans, J.; Pathiaseril, A.; Anderson, A. *J. Am. Chem. Soc.* **1988**, *110*, 5982–5986.

(17) Jorgensen, W. L.; Blake, J. F.; Buckner, J. K. *Chem. Phys.* **1989**, *129*, 193–200.

(18) Lybrand, T. P.; Ghosh, I.; McCammon, J. A. *J. Am. Chem. Soc.* **1985**, *107*, 7793–7794.

(19) Straatsma, T. P.; Berendsen, H. J. C. *J. Chem. Phys.* **1988**, *89*, 5876–5886.

(20) Beveridge, D. L.; DiCapua, F. M. *Annu. Rev. Biophys. Biophys. Chem.* **1989**, *18*, 431–492.

(21) van Gunsteren, W. F. In *Computer Simulation of Biomolecular Systems*; van Gunsteren, W. F., Weiner, P. K., Eds.; Escom: Leiden, 1989; pp 27–59.

(22) Pflugrath, J. W.; Quioco, F. A. *J. Mol. Biol.* **1988**, *200*, 163–180.

(23) Sack, J. S.; Quioco, F. A., unpublished data, 1990.

(24) Hermans, J.; Berendsen, H. J. C.; van Gunsteren, W. F.; Postma, J. P. M. *Biopolymers* **1984**, *23*, 1513–1518.

(25) Berendsen, H. J. C.; Grigera, J. R.; Straatsma, T. P. *J. Phys. Chem.* **1987**, *91*, 6269–6271.

(26) Ryckaert, J. P.; Ciccoliti, G.; Berendsen, H. J. C. *J. Comput. Phys.* **1977**, *23*, 327–341.

(27) Pomès, R.; McCammon, J. A. *Chem. Phys. Lett.* **1990**, *166*, 425–428.

(28) Ben-Naim, A.; Marcus, Y. *J. Chem. Phys.* **1984**, *81*, 2016–2027.

(29) Jorgensen, W. L.; Chandrasekhar, J.; Madura, J. D.; Impey, R. W.; Klein, M. L. *J. Chem. Phys.* **1983**, *79*, 926–935.

good agreement between experimental observations and these preliminary calculations suggests that thermodynamic simulation methods may provide a quantitative approach to determining the thermodynamic properties of protein hydration, although much work must be done to make these methods efficient and simple to use. A complete account of the methods used here, and the thermodynamic and structural changes observed, will be given elsewhere.

Acknowledgment. We thank Professors H. J. C. Berendsen and W. F. van Gunsteren for providing the GROMOS programs and Dr. T. P. Straatsma for helpful discussions. This work was supported by grants from the National Science Foundation, the Robert A. Welch Foundation, the Texas Advanced Research Program, Sterling Drug, the John von Neumann Center, the San Diego Supercomputer Center, the Howard Hughes Medical Institute, and the National Institutes of Health. M.H.M. was supported by the NIH through the Houston Area Training Program in Molecular Biophysics. J.A.M. is the recipient of the George H. Hitchings Award from the Burroughs Wellcome Fund.

Structural and Energetic Evidence for O-Li-N Chelation in a Model for Asymmetric Induction

Edward M. Arnett,* Michael A. Nichols,¹ and Andrew T. McPhail²

Department of Chemistry, Duke University
Durham, North Carolina 27706

Received June 20, 1990

Although controlled synthesis of optically active isomers has been a well-recognized goal of organic chemistry for nearly a century it has only begun to be attained in the last 25 years, primarily through the use of lithium reagents adding to suitably substituted multiple bonds in solvents of low polarity, usually at low temperatures.³ In view of the high charge density of lithium and its resulting tendency to form contact ion pairs, it is very reasonable that the transition structures for stereoselective addition reactions should be controlled by lithium chelation between two adjacent electronegative atoms. Appropriate structures have been proposed for many such cases.⁴

Lithium enolates, amides, and related compounds are highly aggregated in solution⁵ as dimers, tetramers, or even hexamers and X-ray crystal structures have been reported in which lithium

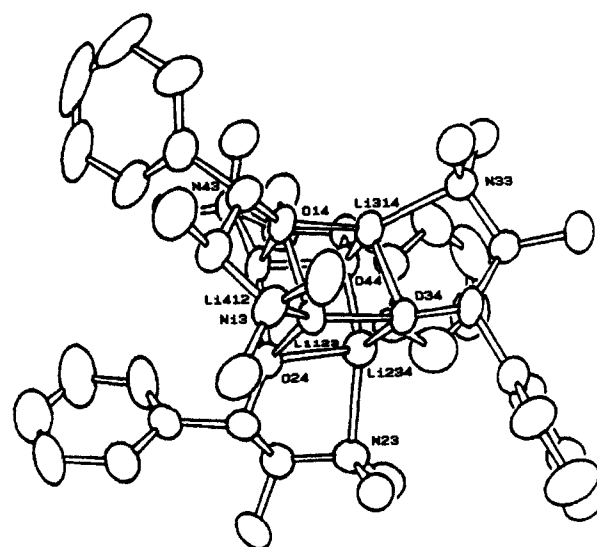


Figure 1. ORTEP diagram of the lithium *N*-methylpseudoephedrate (I) solid-state tetramer. Hydrogen atoms have been omitted for clarity. The Li-O and Li-N bond distances range from 1.870 (13) to 1.985 (13) Å (mean 1.929 Å) and 2.047 (13) to 2.197 (13) Å (mean 2.122 Å), respectively.

Table I. VPO and Cryoscopic Aggregation Numbers (*n*) for Lithium *N*-Methylpseudoephedrate (I) and *N*-Methylephedrate (II) in Benzene and Dioxane^a

compd	<i>n</i> (benzene) ^b	<i>n</i> (dioxane) ^b
I	4.05 ± 0.94 (3.11 ± 1.07)	insoluble
II	4.45 ± 1.02 (3.74 ± 1.67)	5.02 ± 1.31 ^c (5.5 ± 2.5) ^c

^a Cryoscopic results are given in parentheses. ^b Concentrations are 0.150–0.200 *m*. ^c These results indicate that the aggregate is either a tetramer or hexamer.

Table II. Heats of Deprotonation (ΔH_{dep}) for the Alcohols of *N*-Methylpseudoephedrate (I), *N*-Methylephedrate (II), and 2-Methyl-1-phenyl-1-butoxide (III), 2-Methyl-1-phenyl-1-butoxide (IV), and 3-Methyl-1-phenyl-1-butoxide (V) by Lithium Bis(trimethylsilyl)amide (LHMDS) in Benzene and Dioxane at 6 and 13 °C, Respectively^a

alcohol	ΔH_{dep} , kcal/mol	
	benzene ^b	dioxane ^b
I	-33.59 ± 1.38	^c
II	-35.53 ± 0.74	-20.50 ± 1.15
III	-27.15 ± 0.45	-13.58 ± 0.34
IV	-26.22 ± 0.26	-13.21 ± 0.33
V	-27.64 ± 0.80	-14.11 ± 0.76

^a Errors are given at the 95% confidence limit. ^b Corrected for the $\Delta H_{\text{dilution}}$ of HMDMS into benzene and dioxane, +1.30 and +0.97 kcal/mol, respectively. ^c The insolubility of the alkoxide prevented this measurement.

is chelated between appropriately positioned oxygen, nitrogen, and carbon atoms.⁶ To our knowledge, only one series of extensive studies has addressed the actual structures and determined the corresponding energy terms of chelated systems that are directly analogous to the transition structures for asymmetric syntheses employing lithium-controlled chelation.^{4,7}

We have chosen the lithium alkoxides of (-)-ephedrine and (+)-pseudoephedrine, their *N*-methyl derivatives,⁸ and a number

(6) (a) For a review of X-ray structures of organolithium compounds, see: Setzer, W.; Schleyer, P. v. R. *Adv. Organomet. Chem.* **1985**, *24*, 353–450. (b) Footnotes 11–14, 126, 127, 132, and 133 of ref 4g. (c) Jastrzebski, J. T. B. H.; van Koten, G.; van de Meiroop, W. F. *Inorg. Chim. Acta* **1988**, 169–171. (d) Moene, W.; Schakel, M.; Hoogland, J. M.; de Kanter, F. J. J.; Klumpp, G. W. *Tetrahedron Lett.* **1990**, *31*, 2641–2642, and refs 6 and 7 therein. (7) For a pioneering study, see: Beak, P.; Seigel, B. *J. Am. Chem. Soc.* **1974**, *96*, 6803–6805.

(1) From the projected Ph.D. dissertation of Michael A. Nichols, Duke University, 1990.

(2) Duke University Structure Center.

(3) (a) Morrison, J. D.; Mosher, H. S. *Asymmetric Organic Reactions*; Prentice-Hall: Englewood Cliffs, NJ, 1971. (b) *Asymmetric Syntheses*; Morrison, J. D., Ed.; Academic Press: New York, 1983; Vols. 2, 3. (c) Eliel, E.; Otsuka, S. *Asymmetric Reactions and Processes in Chemistry*; ACS Symposium Series 185; American Chemical Society: Washington, DC, 1982. (d) Mosher, H. S.; Morrison, J. D. *Science* **1983**, *221*, 1013–1019.

(4) (a) Beak, P.; Reitz, D. B. *Chem. Rev.* **1978**, *78*, 275–316. (b) Beak, P.; Zajdel, W. J.; Reitz, D. B. *ibid.* **1984**, *84*, 471–523. (c) Meyers, A. I. *Aldrichimica Acta* **1985**, *18*, 59–68. (d) Meyers, A. I. *Lect. Heterocycl. Chem.* **1984**, *7*, 75–81. (e) Meyers, A. I.; Dickman, D. A.; Boes, M. *Tetrahedron* **1987**, *43*, 5095–5108. (f) Meyers, A. I.; Knaus, G.; Karnata, K. J. *Am. Chem. Soc.* **1974**, *96*, 268. (g) Beak, P.; Meyers, A. I. *Acc. Chem. Res.* **1986**, *19*, 356–363. (h) Lutomski, K. A.; Meyers, A. I. *Asymmetric Synthesis via Chiral Oxazolines*. In *Asymmetric Syntheses*; Morrison, J. D., Ed.; Academic Press: New York, 1983; Vol. 3, pp 213–274. (i) Enders, D. Alkylation of Chiral Hydrazones. In *Asymmetric Syntheses*; Morrison, J. D., Ed.; Academic Press: New York, 1983; Vol. 3, pp 275–339. (j) Klumpp, G. W. *Recl. Trav. Chim. Pays-Bas* **1986**, *105*, 1–21, and references therein. (k) See, however: Das, G.; Thornton, E. R. *J. Am. Chem. Soc.* **1990**, *112*, 4350–4362.

(5) (a) For an excellent review, see: Seebach, D. *Angew. Chem. Int. Ed. Engl.* **1988**, *27*, 1624–1654. (b) Jackman, L. M.; Smith, B. D. *J. Am. Chem. Soc.* **1988**, *110*, 3829–3835, and references therein. (c) DePue, J. S.; Collum, D. B. *J. Am. Chem. Soc.* **1988**, *110*, 5518–5524, and references therein. (d) Arnett, E. M.; Fisher, F. J.; Nichols, M. A.; Ribeiro, A. A. *J. Am. Chem. Soc.* **1990**, *112*, 801–808.